http://journal.uir.ac.id/index.php/JGEET

E-ISSN : 2541-5794
P-ISSN : 2503-216X

Journal of Geoscience,
Engineering, Environment, and Technology
Vol 10 No 04-2/2025

RESEARCH ARTICLE

Integrated Analysis of Seismic and Well Data to Determine CO_2 Injection Zones in "W" Field of The Talang Akar Formation, Asri Basin

Muhammad Feri Edo Ardiansyah [1], M. Husni Mubarak Lubis [1,*]
[1] Department of Geophysical Engineering, Faculty of Technology Exploration and Production, Universitas Pertamina, Jakarta, 12220, Indonesia

* Corresponding author : muhammad.hml@universitaspertamina.ac.id
Tel.: 62 812-2256-8918
Received: Jul 31, 2025; Accepted: Jan 9, 2026.
DOI: 10.25299/jgeet.2025.10.1.1.24363

Abstract

Asri Basin is one of the most prospective areas to store CO_2 in a CCS project in Indonesia. Previously, Asri basin was one of the most prolific oil and gas provinces in the region. This study characterizes the CO_2 injection zone in the saline aquifer reservoir by analyzing seal, storage, and injectivity. A model-based seismic inversion method was used to produce an acoustic impedance volume, which was then transformed into a porosity volume and a permeability volume. Also, analysis of seismic variance attributes was also carried out to investigate the presence of faults surrounding the seal. The results indicated that the seal quality criteria in the study area are satisfactory because no faults intersect the seal. The average distribution of porosity values in the injection target zone is 32%, with the distribution of permeability values being more than 500 mD, making the area satisfactory for CO_2 injection.

Keywords: Model-Based Inversion, Seal Storage, Injectivity, Saline Aquifer

1. Introduction

1.1 Background of Research

One of the efforts to promote CCS in Indonesia is to develop CCS Hubs in Sunda-Asri Basin. Asri Basin is located on the north coast of West Java (**Figure 1**), an area with relatively stable tectonics, making it preferable for CCS implementation and minimizing the risk of seal leakage due to tectonic activities. This study aims to characterize the reservoir in the target area of the CCS site, namely the "W" field, Asri Basin. "W" is a highly mature oil field that has been in production since 1990 with cumulative oil production of nearly 400 MMSTB. The reservoirs are fluvial-deltaic sandstones of The Upper Talang Akar Formation (TAF), primarily consisting of the Gita Member and Upper Zelda Sandstones (Ravizon et al., 2025).

This study utilizes Acoustic Impedance (AI) integrated with well data analysis. AI obtained from the multiplication between density and P wave velocity can be used to derive porosity. The relationship between porosity and permeability is observed from the crossplot of core data. The acoustic impedance cube is obtained from model-based seismic inversion; it was then used to obtain a porosity model and a permeability model to determine the potential zone of CO_2 injection in the "W" field, Asri Basin, for Carbon Capture Storage (CCS) purposes. Petrophysical analysis and core data were also carried out to further understand reservoir properties, such as porosity analysis, water saturation, and volume of shale.

1.2 Reservoir Assessment Criteria

Figure 2 illustrates the stratigraphy of the Asri Basin from the Banuwati Formation to the Cisubuh Formation. The Baturaja Formation and the Gumai Formation in the Asri Basin act as regional seals. Meanwhile, the reservoir in the Asri Basin is the Talang Akar Formation, with the Gita and Zelda Members being the main reservoir (Sukanto et al., 1998). The reservoir is interpreted as a compartmentalized meandering channel characterized by a clean and blocky pattern of gamma ray logs. A detailed study about the geometry of the channel from seismic data has been documented by Carter et al. (1998) and Muliani et al. (2018).

According to Halland et al. (2013), the quality of the seal is considered good if it meets the criteria presented in **Table 1** and **Table 2**. The reservoir should have more than one formation that acts as a seal, a thickness greater than 100 meters, a high clay content, no faults, no fractures, and no wells that penetrate the seal in the CO_2 injection target zone. Meanwhile, a reservoir is considered satisfactory if it meets the following criteria: has traps in the form of seals that act as a cover to prevent CO_2 leakage to the surface, is not located in the overpressure zone, has a reservoir depth of >800 meters, has a reservoir thickness of >50 meters with a porosity of >25%, and has a permeability of >500 mD.

In the selection of the target reservoir, the CO_2 injection zone must be more than 800 meters, because at that depth the injected CO_2 will experience high pressure and temperature, as shown in **Figure 3**. At a depth of > 800 meters, CO_2 will experience a supercritical phase at a temperature of 304 Kelvin or 31.1°C with a pressure of 7.38 MPa. In this phase, the gas will have a higher density than the usual gas. This results in a larger storage capacity, as CO_2 can be stored in smaller volumes and at higher densities.

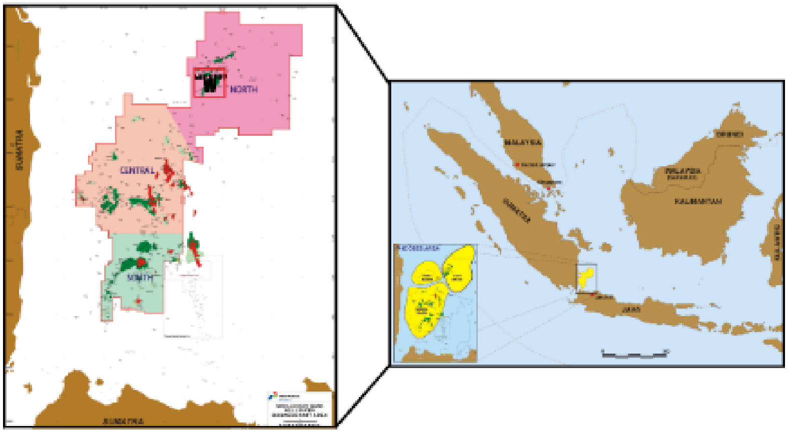

Fig. 1. The location map of the research area is indicated by a red box (PHE OSES)

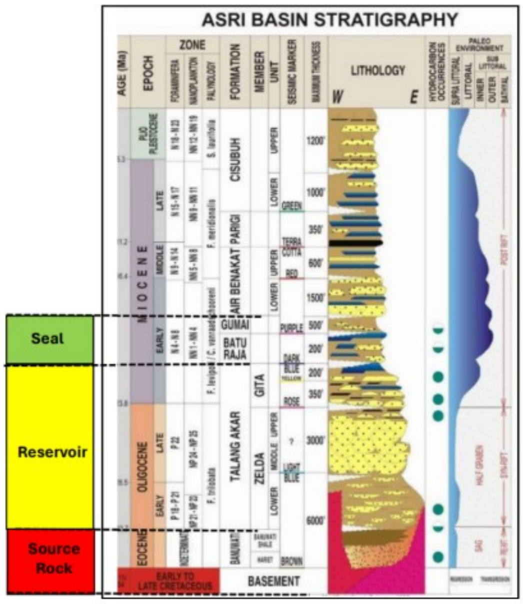

Fig. 2. Stratigraphy of the Asri Basin (Ralanarko et al., 2021)

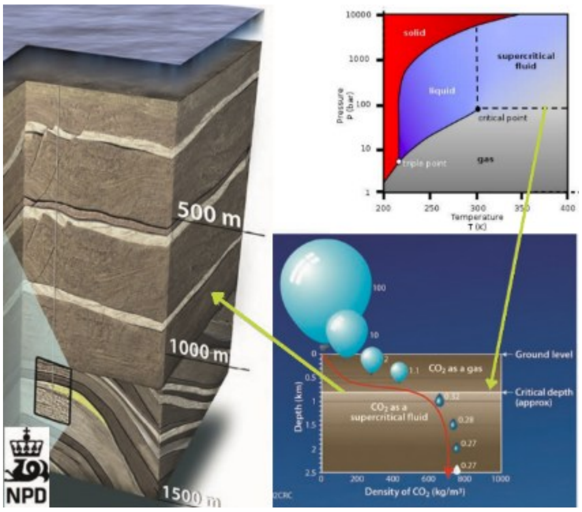

Fig. 3. Super-Critical Fluid Phase (Davis et al., 2019)

Table 1. The Reservoir-Assessment Criteria: Typical High and Low Scores

Reservoir Properties	High Scores	Low Scores
Traps	Defined sealed structures	Poor definition of traps
Pore pressure	Hydrostatic or lower	Overpressure
Depth	> 800 m	< 800 m
Net thickness	> 50 m	< 15 m
Average porosity in net reservoir	> 25%	< 15%
Permeability	> 500 mD	< 10 mD

Table 2. The Seal-Assessment Criteria: Typical High and Low Scores

Sealing Properties	High Scores	Low Scores
Sealing layer	> 1	1
Properties of seal	> 100 m thickness	< 50 m
Composition of seal	High clay content	Silty or silt layers
Faults	No fault through the seal	Big throw through seal
Other breaks through seal	No fracture	Sand injection, slumps
Well (exploration / production)	No drilling through seal	High number of wells

2. Data and Method

2.1 Data

In this study, various data are utilized including seismic data, log data, checkshot data, well tops data, horizon data, and core data.

Seismic Data. Using 3D seismic post-stack data in SEGY format, with detailed information from the seismic data used is as follows.

- Inline: 350 – 1248
- Crossline: 180–1160
- Sampling rate: 1 ms
- Polarity: SEG Reverse
- Time Window: 0–3000 ms

Log Data. This study uses data from four wells: W-1, W-4, W-6, and W-10, and the completeness of the log data is presented in **Table 3**.

Checkshot Data. The checkshot data in this study is available on all wells that will be used to perform checkshot correction to correct and correlate seismic data with well data.

Well Tops Data. Well top data provides information on top of each formation. Well top data is important for the purpose of the well-to-seismic tie process and horizon interpretation. In this study, there are three well tops used, namely Gumai, TAF (Talang Akar Formation), and Top Zelda.

Horizon Data. In this study, horizon interpretation data was provided, such as 1) The horizon of Gita refers to the top of the Talang Akar formation, which serves as the uppermost reservoir; 2) Horizon Orange is at the top of the Zelda formation; and 3) Horizon of Basement.

Core Data. This study has core data on several wells, including the W1 well and the W10 well.

2.2 Method

The workflow of the entire process is shown in **Figure 4**. Data processing that will be carried out in this study consists of several main stages.

Wavelet Extraction. The wavelet extraction process must be completed before performing a well-to-seismic tie and inversion. In this study, the estimation of wavelets was carried out through the extraction process of seismic data in the zone around the target zone. The selection of wavelet length is based on a calculation that ranges from 1/3 to 1/7 of the window width, as proposed by Carvajal et al. (2022).

Fault Interpretation. Fault interpretation is carried out to determine faults in the study area marked by discontinuity of seismic reflectors. The fault interpretation process in this study was carried out in all areas in the target zone. The purpose of the fault interpretation in this study is to select the zone where CO_2 injection will be carried out with no faults passing through the seal or the deep saline aquifer zone in the reservoir to avoid leakage of CO_2.

Table 3. Data Availability of Log Data

Sumur	Log Data							Core Data	Posisi Sumur Terhadap Data Seismic	
	GR	VP	VS	RES	RHOB	NPHI	CAL		Inline	Crossline
W-1	✓	✓	–	✓	✓	✓	✓	✓	964	658
W-4	✓	✓	–	✓	✓	✓	✓	–	860	732
W-6	✓	✓	–	✓	✓	✓	✓	–	1142	499
W-10	✓	✓	–	✓	✓	✓	✓	✓	648	609

Keterangan: ✓ = data tersedia; – = data tidak tersedia

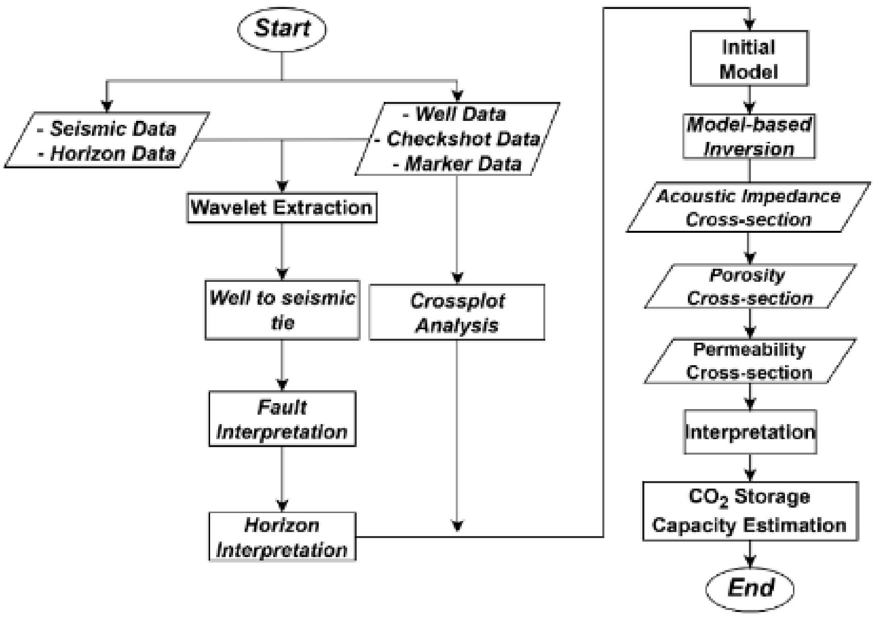

Fig. 4. Flowchart of Reservoir Characterization Process

Crossplot Analysis. The sensitivity test process is carried out to determine the sensitive parameters of the well log data. Based on these sensitive parameters, a cut-off value will be obtained to determine the distribution of lithology and fluids in reservoir characterization by cross plotting between acoustic impedance and porosity log data in the target zone, starting from the top Zelda marker to the bottom Zelda.

Initial Model. The initial model is done by applying a low-pass filter to AI information obtained from the log. The filtered AI from the log is then extrapolated within the field using the inverse distance algorithm.

Model-Based Inversion. The seismic inversion process was performed using a model-based approach. Model-based seismic inversion is an iterative approach that begins by constructing an initial impedance model to be compared against observed seismic data. In this process, a synthetic seismic response is calculated from the model and compared with the original data; if discrepancies (errors) exist, the impedance model is updated iteratively until the optimal fit between the model, and the data is achieved (Russell, 1988).

3. Results and Discussion

3.1 Well Log Analysis

Petrophysical analysis of wells W-1, W-4, W-6, and W-10 are shown in **Figure 5**. Based on the gamma ray log, it is found that each well has a sand reservoir saturated with water, shown by the black box line with varying reservoir thickness. In addition, in wells W-1 and W-10 there is core porosity data shown by the blue tadpole on track 4 **Figure 5A** and **Figure 5D**, which are juxtaposed with the estimated porosity log. Based on the comparison between the porosity log and the porosity core data, the porosity log estimates show the same trend as the porosity core data, so it can be said that the results of the porosity log calculation are correct.

The sandstone reservoir exhibits a blocky to bell-shaped fining upward profile that indicates fluvial channel sedimentation with varying thickness. This result is aligned with the well log analysis of Sukaryadi (2002) that shows porosities range from 32.9% to 39.4%, while core permeabilities extend from 3,511 mD to 10,690 mD.

3.2 Crossplot Analysis

Figure 6 and **Figure 7** show the results of AI between show and porosity using 2 different color keys, namely Gamma ray and water saturation. Based on the crossplot analysis in **Figure 6**, a cutoff is obtained to separate the sand and coal. The yellow box shows the sand lithology, which has a low Gamma ray value of <50 API with an acoustic impedance value of 16800 - 23000 (ft/s)*(g/cc) and has a porosity ranging from 26% to 38%. While coal has an acoustic impedance value of less than 16800 ft/s * g/cc with a higher total porosity of more than 38%. Coal has low density that makes it seem to have higher total porosity compared to sandstones. The equation in Figure 6 will later be used to convert from acoustic impedance to porosity. **Figure 7** shows that the sand lithology in the yellow box is a reservoir saturated with water.

This field is used to be a prolific oil and gas field in the region. Now, the oil and gas are not produced anymore from the reservoir. Therefore, the reservoir is now fully saturated with water, making it suitable for CO_2 injection.

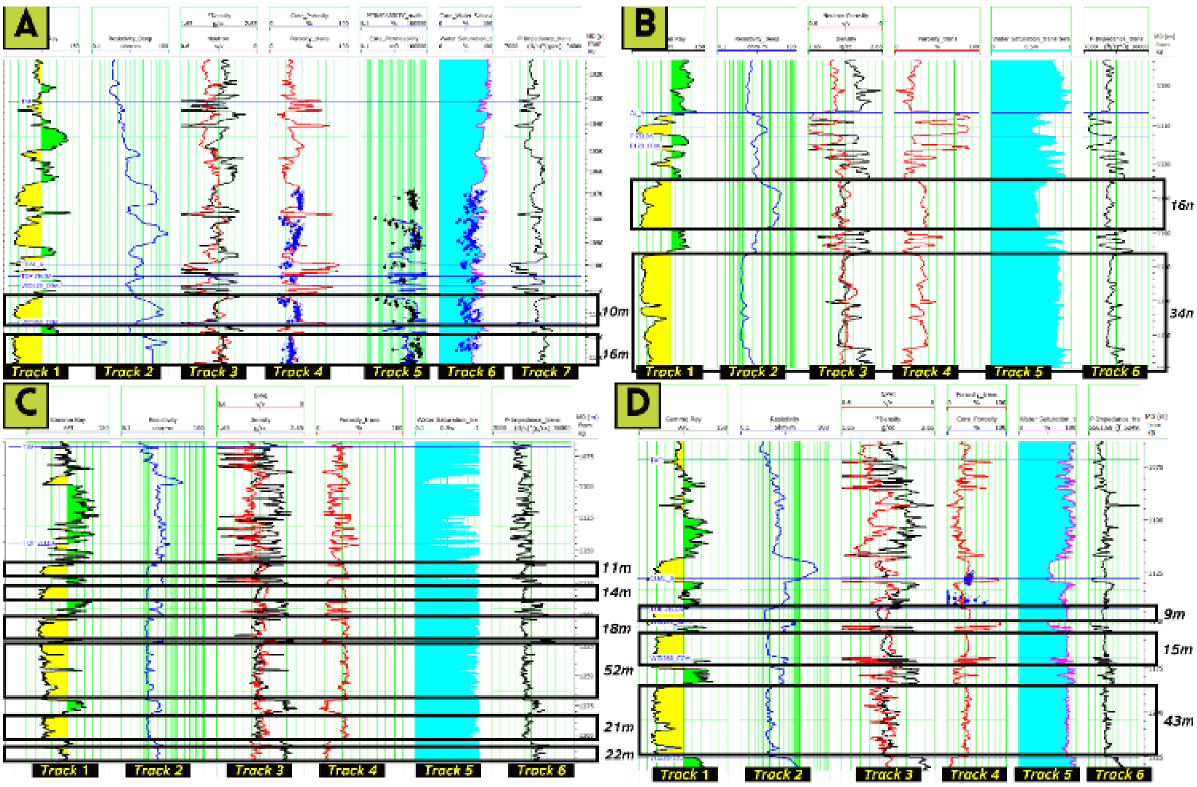

Fig. 5. Analysis of the Target Zone at W-1 (A), W-4 (B), W-6 (C), and W-10 (D)

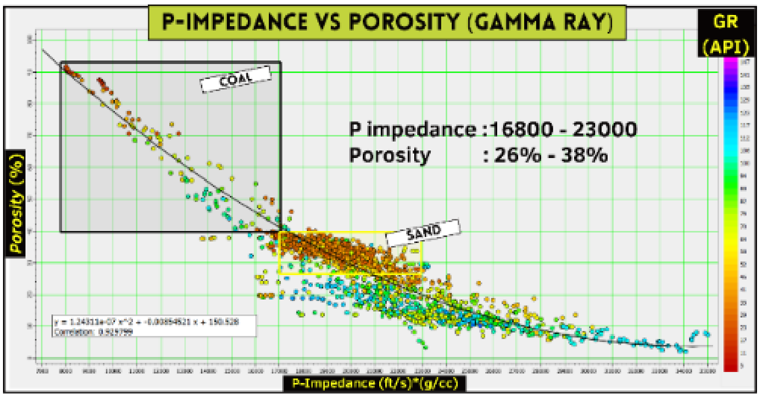

Fig. 6. Crossplot of Acoustic Impedance vs. Porosity (color key GR)

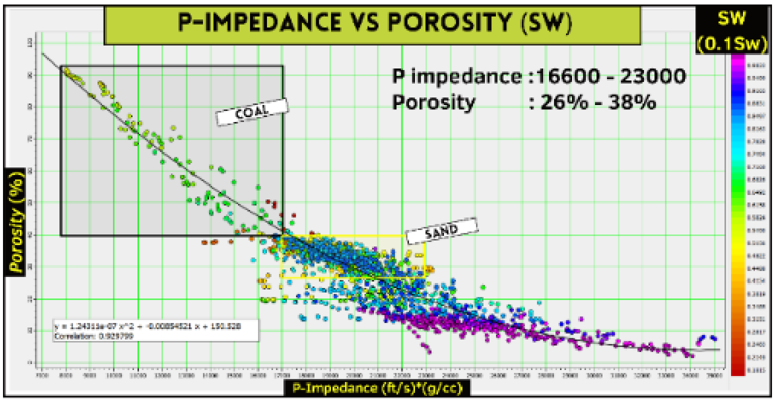

Fig. 7. Crossplot of Acoustic Impedance vs. Porosity (color key SW)

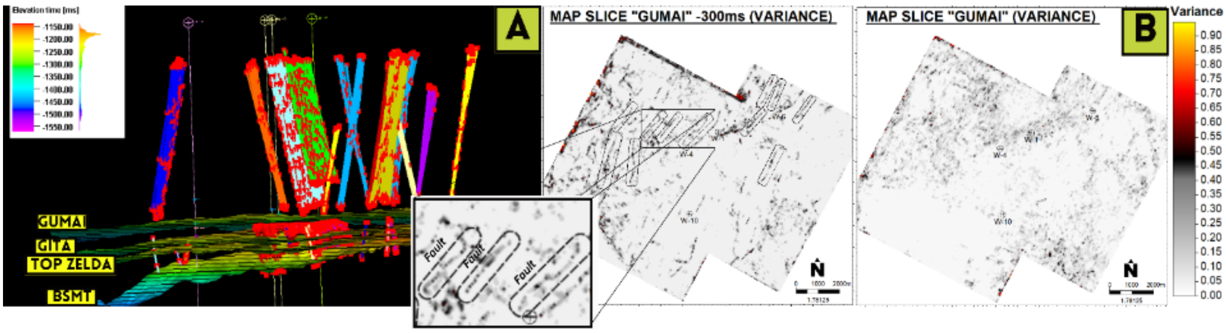

Fig. 8. (A) Fault Interpretation (B) Variance Attribute 300ms above (left) and exactly (right) at Gumai Formation

3.3 Fault Interpretation

Fault interpretation was carried out in all areas with the aim of identifying the presence of faults that pass through the seal. Based on **Figure 8** (A), the results show that there are 18 faults identified, where all of these faults do not penetrate the Gumai formation. **Figure 8** (B) shows that the seismic variance attribute is applied both at the Gumai Formation and 300 ms above it. It can be seen that the variance attribute generated exactly at Gumai formation does not find any linear high-variance patterns that indicate the presence of faults. Whereas in the 300 ms slicing above the Gumai formation, there are several linear high variance patterns that indicate the presence of a fault above Gumai formation. Detailed seismic attribute studies in the W field to highlight structural features were performed by Carter et al. (1998) and (2002).

The analysis of seismic variance attributes indicates that there are no faults that penetrate the seal. However, there are several production wells that penetrate the reservoir. Further investigation regarding well integrity is required to further understand whether these pre-existing productions can be converted to CO_2 injectors.

3.4 Acoustic Impedance Model-Based Inversion

The distribution of acoustic impedance values is in the range 13839 - 27000 (ft/s)*(g/cc), as shown in **Figure 9**. It can be seen that the distribution between the acoustic impedance inversion results and the acoustic impedance from the well already has a matching color, indicating that the inversion results obtained are satisfactory.

In this study, a crossplot has been obtained to show the impedance value for sandstone saturated with > 60% of water with an acoustic impedance value of 16600–23000 (ft/s) * (g/cc).

3.5 Porosity Cross-Section Analysis

Figure 10 shows the result of the distribution of porosity values ranging from 0 to 65%. **Figure 12** is a cross section of the distribution of porosity values that have been filtered on the color bar, namely with a value of 26 - 38%, with the assumption that the porosity in that range is clean sand lithology saturated with water that has been obtained through the previous crossplot analysis. While the area with porosity > 38% indicates coal. In **Figure 11**, the initial targeted area that will be used as a prospect for CO_2 injection is also determined, which is shown by the black dotted line in the figure. The selection of the CO_2 injection target zone was carried out just below the Top Zelda to Middle Zelda formation.

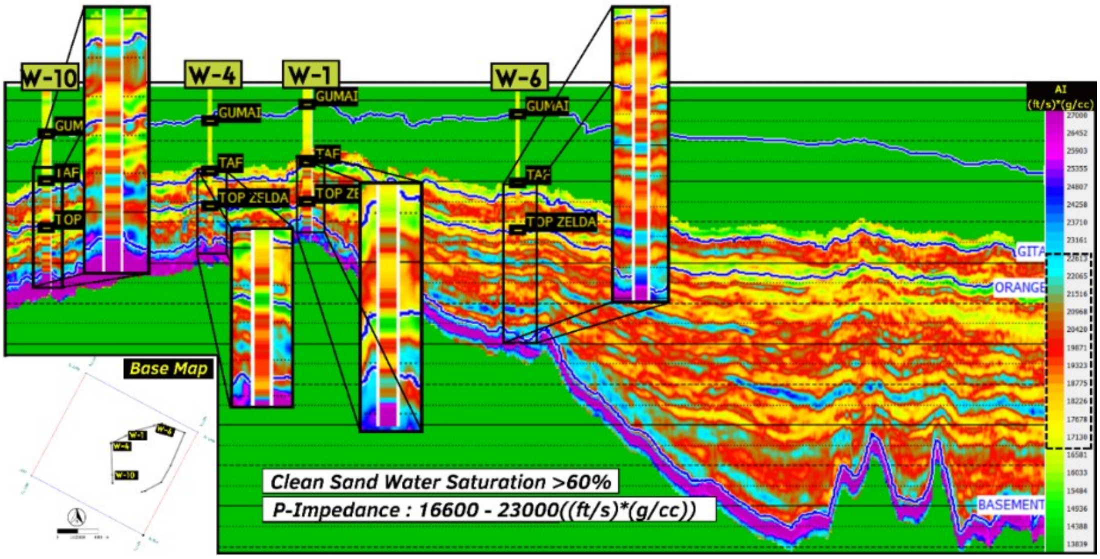

Fig. 9. Acoustic Impedance Cross Section

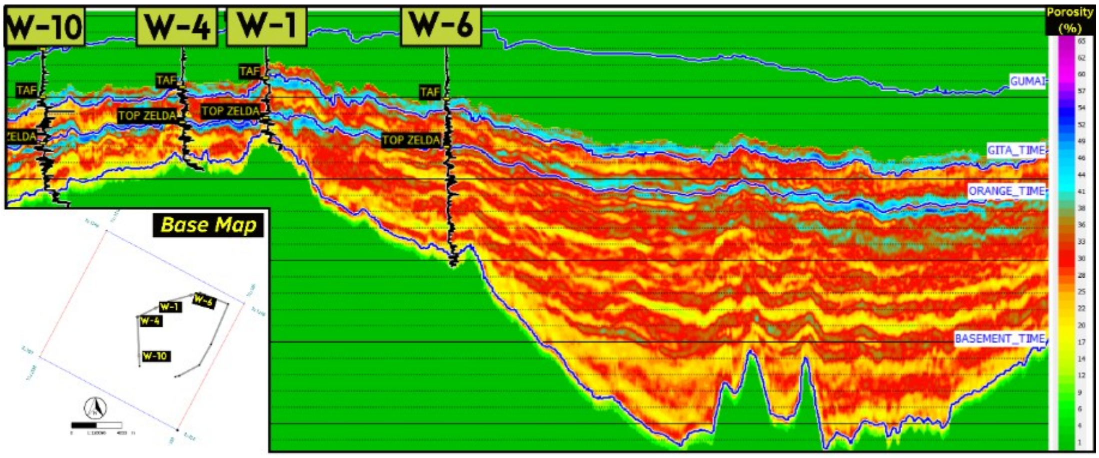

Fig. 10. Cross-section of Porosity Distribution

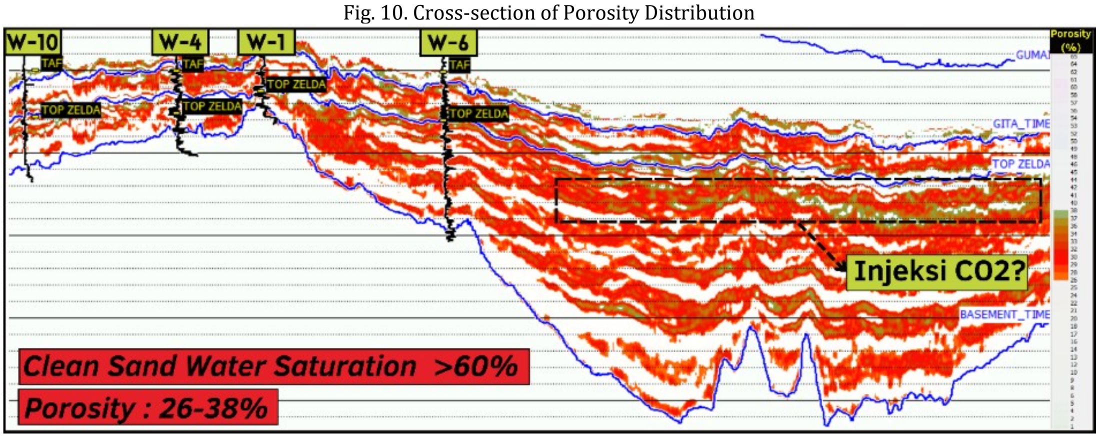

Fig. 11. Cross-section of Porosity Distribution (filtered for coal presence)

3.6 Permeability Cross-section Analysis

The permeability value cross section is used to see the distribution of permeability values in the CO_2 injection target zone, where the criteria used for analyzing the quality of excellent CO_2 injection reservoirs have permeability values > 500 mD. **Figure 12** and **Figure 13** show the results of the permeability value distribution cross section obtained. Based on these results, permeability has a value in the range of 10 to 100,000 mD. The CO_2 injection target zone, indicated by the black dotted line, has a permeability value ranging from log(2.7), which is 501.1 mD, to log(4), which is 10000 mD. The cutoff on the colorbar permeability value is not more than log(4) because the unrealistically higher permeability value more than that is the effect of coal, which results from the low-density nature of coals.

3.7 Slicing Map

Map slicing was carried out on the target zone for CO_2 injection that has been determined in the Top Zelda formation + 40 ms down, which is carried out on the volume of acoustic impedance, porosity, and permeability as shown in **Figure 14** and **Figure 15**. The results of the slicing map indicate that the CO_2 injection target zone, represented by the polygon with a black dotted line, has an acoustic impedance value ranging from 16600 to 23000 (ft/s)*(g/cc), a porosity of 26 to 38%, which corresponds to a clean sand lithology that is saturated with water, and a permeability in the injection zone exceeding 500 mD. Where, based on the distribution values of porosity and permeability obtained, the CO_2 injection zone is categorized as having good storage with porosity > 25% and adequate injectivity with permeability > 500 mD.

Figure 16 displays the slicing map results alongside the fault interpretation for the target horizon, indicating that there are no faults penetrating the CO_2 injection target reservoir area.

4. Conclusion

The results of the seal quality analysis based on predetermined criteria show that the seal quality is a good criterion for CO_2 injection in the application of Carbon Capture and Storage (CCS). In Table 4, the criteria are met, including consisting of more than 1 formation that acts as a seal, namely the Gumai formation and Batu Raja; having an average seal thickness of 120 meters; and having no faults that penetrate the seal.

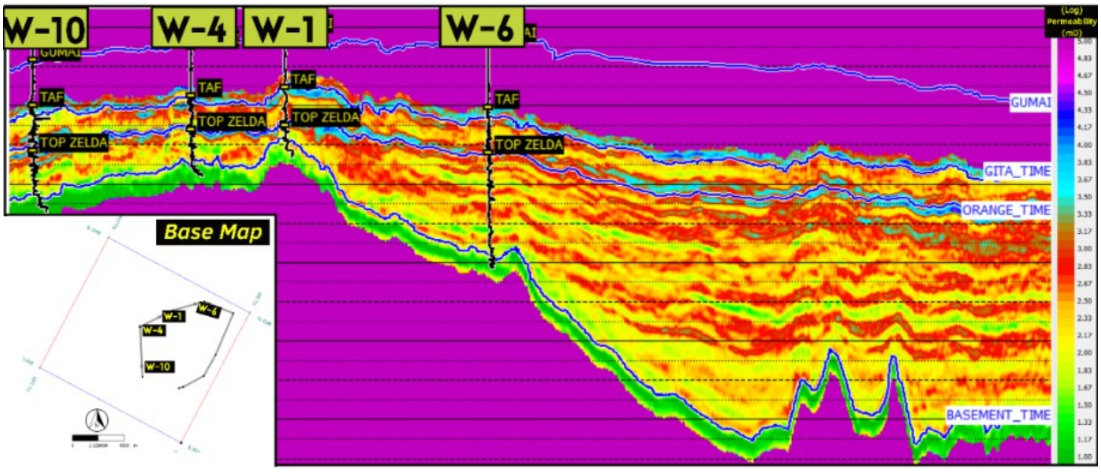

Fig. 12. Permeability Distribution Cross-section

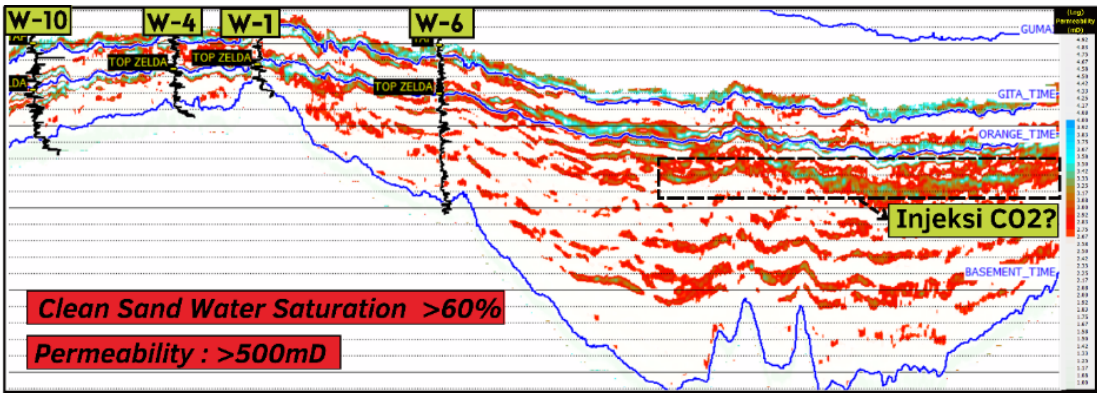

Fig. 13. Permeability Distribution Cross-section (filtered for coal presence)

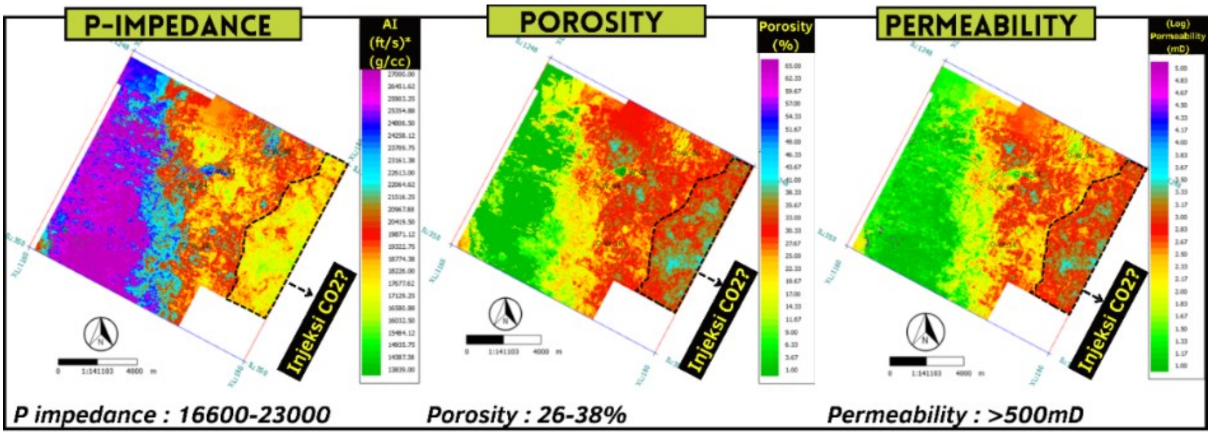

Fig. 14. Slicing Map Acoustic Impedance, Porosity, Permeability

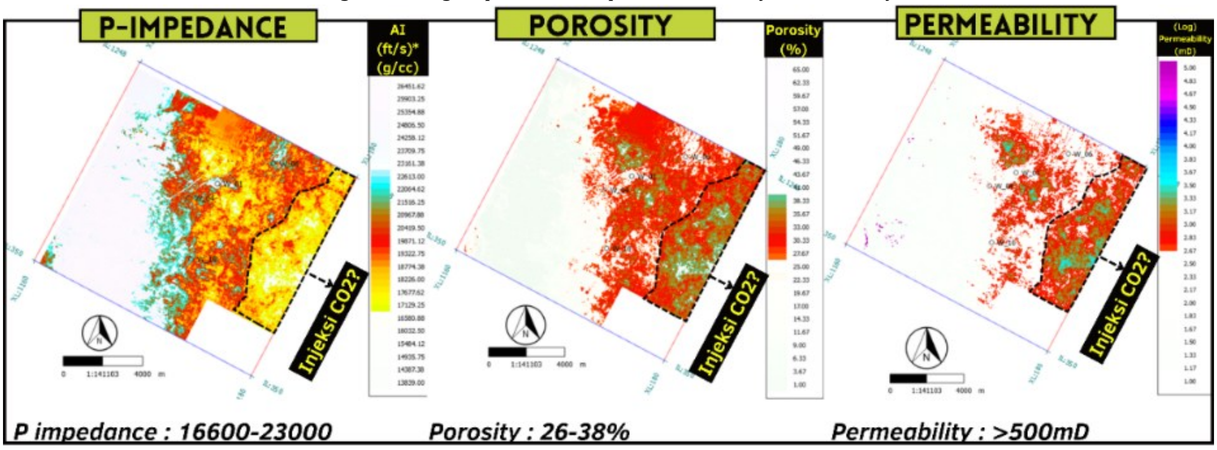

Fig. 15. Slicing Map Acoustic impedance, porosity, permeability (filtered for coal)

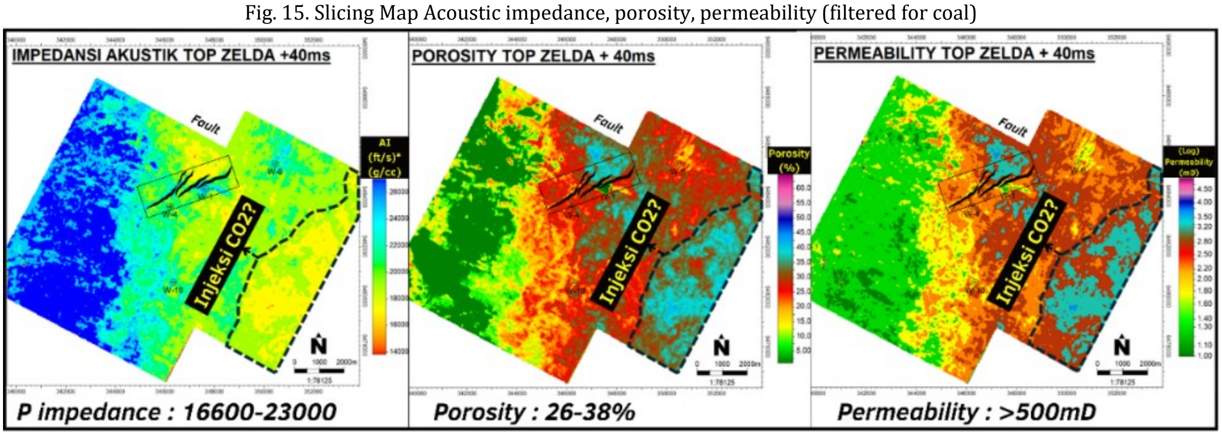

Fig. 16. Slicing Map Acoustic Impedance, Porosity, Permeability

The acoustic impedance inversion approach yields an average porosity value of 32% in the CO_2 injection target zone, which meets acceptable criteria for CO_2 injection, as it represents the porosity of clean sand lithology saturated with water. Based on this distribution, the porosity value in the injection target reservoir exceeds 25%, which meets the criteria for satisfactory storage for CCS.

The average permeability value obtained in the CO_2 injection target zone reservoir is 1995 mD. Therefore, the target zone area for CO_2 injection meets the criteria for a good permeability assessment for carbon capture and storage, which is greater than 500 mD.

Acknowledgements

The authors would like to thank Pertamina Hulu Energi Offshore Southeast Sumatera (PHE OSES) for providing the data and fruitful discussion for this study. The authors also would like to thank Geosoftware and SLB for providing the essential tools that facilitated the data analysis, contributing significantly to the successful completion of this research.

Data and Material Availability

Data and material associated with this study are confidential and cannot be released.

References

Carter, D.C., Armon, J., Harmony, W.E., Himawan, R.S., Lukito, P., Syarkawi, I. and Tonkin, P.C., 1998. Channel and sandstone body geometry from 3D seismic and well control in Widuri Field, offshore SE Sumatra, Indonesia. In: Proceedings of the Indonesian

Petroleum Association, Twenty-Sixth Annual Convention, May 1998.
Carter, D.C., Harmony, W.E., Harvidya, L., Juniarto, G., Lestari, S. and Purba, A., 2002. Seismic interpretation methodology for fluvial sandstone reservoirs. In: Proceedings of the Indonesian Petroleum Association, Twenty-Eighth Annual Convention & Exhibition, Vol. 1.
Carvajal, C., Fernandez, J. and Aristimuno, J., 2022. Well tie tutorial and its importance in seismic interpretation and inversion.
Davis, T.L., Landrø, M. and Wilson, M. (eds.), 2019. Geophysics and geosequestration. Cambridge: Cambridge University Press. https://doi.org/10.1017/9781316480724
Halland, E.K., Riis, F., Magnus, C., Johansen, W.T., Tappel, I.M., Gjeldvik, I.T. and Pham, V.T.H., 2013. CO_2 storage atlas of the Norwegian part of the North Sea. Energy Procedia, 37, pp.4919–4926. https://doi.org/10.1016/j.egypro.2013.06.403
Muliani, R., Widiatmo, R., Gunawan, H., Nugroho, P., Hairunnisa, M.A. and Saputra, R., 2018. New approach: using relative inversion with spectral decomposition to distinguish thin layers in the 33-series sand reservoirs of the Widuri Field, Southeast Sumatra, Indonesia. In: Proceedings of the Indonesian Petroleum Association, Forty-Second Annual Convention & Exhibition, May 2018. https://doi.org/10.29118/IPA18.10.G
Ralanarko, D., Ramadhan, M.I., Fauzielly, L. and Syafri, I., 2021. Asosiasi fasies dan rekonstruksi paleogeografi pada zona transisi Formasi Talangakar, Cekungan Asri, lepas pantai Blok Tenggara Sumatra, Indonesia. Jurnal Geologi Kelautan, 19(2). https://doi.org/10.32693/jgk.19.2.2021.736
Ravizon, Y., Nugroho, P., Dondo, M., Tumanggor, P. and Winiarti, 2025. Low quality reservoir development of Upper Talang Akar Formation shaly sand reservoir in Widuri Field, Southeast Sumatra. In: Proceedings of the Indonesian Petroleum Association, Forty-Ninth Annual Convention & Exhibition, May 2025.
Russell, B.H., 1988. Introduction to seismic inversion methods. Tulsa, OK: Society of Exploration Geophysicists. https://doi.org/10.1190/1.9781560802303
Sukanto, J., Nunuk, F., Aldrich, J.B., Rinehart, G.P. and Mitchell, J., 1998. Petroleum systems of the Asri Basin, Java Sea, Indonesia. In: Proceedings of the Indonesian Petroleum Association, Twenty-Sixth Annual Convention.
Sukaryadi, E.K.A., 2002. Characteristics and sandbody geometry of the 34-1 reservoir, Widuri Field offshore Southeast Sumatra. In: Proceedings of the Indonesian Petroleum Association, Twenty-Eighth Annual Convention & Exhibition, Vol. 1.